On the Formation Mechanism for Electrically Generated Exciplexes in a Carbazole–Pyridine Copolymer

Anna Hayer,[1,2]* Tanguy Van Regemorter,[3] Bianca Höfer,[1§] Chris S. K. Mak,[4†] David Beljonne,[3] Anna Köhler[1]

[1]Experimental Physics II and Bayreuth Institute for Macromolecular Research (BIMF), University of Bayreuth, Universitätsstr. 30, 95448 Bayreuth, Germany

[2]Cavendish Laboratory, University of Cambridge, JJ Thompson Avenue, Cambridge CB3 OHE, United Kingdom

[3]Laboratory for Chemistry of Novel Materials, University of Mons, Place du Parc 20, B-7000 Mons, Belgium

[4]Department of Chemistry, University of Cambridge, Lensfield Road, Cambridge CB2 1EW, United Kingdom

Correspondence to: A. Köhler (E-mail: anna.koehler@uni-bayreuth.de)

Received 12 October 2011; revised 14 November 2011; accepted 15 November 2011; published online 13 December 2011
DOI: 10.1002/polb.23011

ABSTRACT: Although carbazole-containing copolymers are frequently used as hole-transporting host materials for polymer organic light-emitting diodes (OLEDs), they often suffer from the formation of undesired exciplexes when the OLED is operated. The reason why exciplexes sometimes form for electrical excitation, yet not for optical excitation is not well understood. Here, we use luminescence measurements and quantum chemical calculations to investigate the mechanism of such exciplex formation for electrical excitation (electroplex formation) in a carbazole–pyridine copolymer. Our results suggest that the exciplex is formed via a positively charged interchain precursor complex. This complex is stabilized by interactions that involve the nitrogen lone pairs on both chain segments. © 2011 Wiley Periodicals, Inc. J Polym Sci Part B: Polym Phys 50: 361–369, 2012

KEYWORDS: charge transfer; light-emitting diodes (LED); luminescence; photophysics; quantum chemistry; UV–vis spectroscopy

INTRODUCTION Organic semiconductor materials are used for the fabrication of opto-electronic devices such as organic light-emitting diodes (OLEDs) and solar cells. Today's state-of-the-art devices typically contain an active layer that comprises several components, each of them optimized for different functions. Solar cells are made by blending hole accepting/transporting materials with electron accepting/transporting materials,[1–8] whereas OLEDs contain at least a hole transporting compound, an electron transporter, and, sometimes, an emitter molecule.[9–11] The performance of such devices is controlled by the physical processes that take place at the internal interfaces between two materials. It is, therefore, necessary to get a thorough understanding of such intermolecular interactions.

An intermolecular process that is of central importance to the operation of OLEDs consists in the formation of excimers or exciplexes, that is, excited states that extend over two identical or dissimilar molecules, respectively.[12,13] Sometimes, excimers and exciplexes are only observed for electrical excitation, that is, by charge recombination in a OLED, and not for optical excitation. In this case, they are referred to as electromers or electroplexes. Although there are numerous reports concerning the observation of electroplexes,[14–22] surprisingly little is known about their formation pathway.

When considering the literature, it is noticeable that electroplexes and exciplexes are reported in particular for materials that contain a nitrogen atom in certain moieties. For example, electroplexes are known for combinations of organic semiconductors that contain carbazole-moieties, amine-moieties, oxadiazole-moieties, and other diazole-moieties.[14–22] The same type of materials are also prone to exciplex formation. Exciplexes are found in polymers containing oxadiazole and triphenylamine substitutens,[23] fluorene-benzothiadiazole copolymer (F8BT) and fluorene-triphenyldiamine copolymer (PFB),[11,13] cyano-substituted poly(p-phenylene vinylene) polymer (CN-PPV)s,[5–7] polyquinolines, polyimines, and polymers containing pyridine-units.[12,24,25] Compounds with nitrogen-containing moieties are frequently used as charge-transport materials for device applications. An understanding of the factors that

*Present address: Merck KgaA, Darmstadt, Germany.
†Present address: Chris S. K. Mak, Department of Chemistry, The University of Hong Kong, Pokfulam Road, Hong Kong, China.
§Present address: Bianca Höfer, IFW-Dresden, Dresden, Germany.

Additional Supporting Information may be found in the online version of this article.

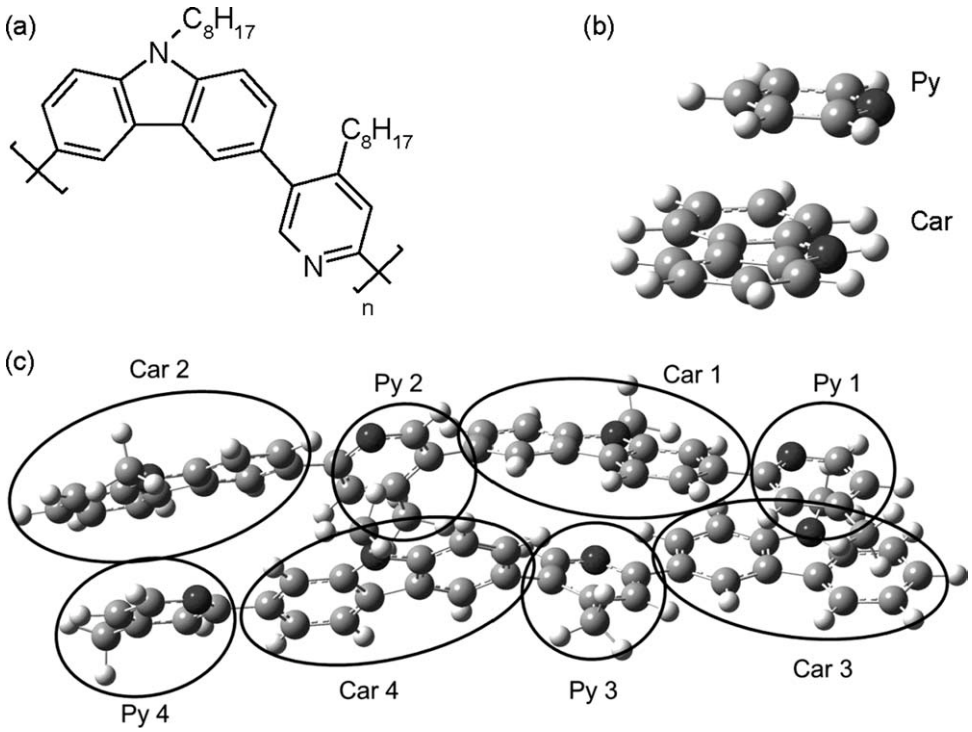

FIGURE 1 Chemical structure of (a) the polymer Car-Py (carbazole linked to a pyridine unit) used for the experiments, (b) the individual carbazole and pyridine moiety used as model system in the theoretical investigation, and (c) the two dimers used as model system in the theoretical investigation. For reference, the different carbazole and pyridine units have been indicated.

contribute to the formation of exciplexes in operating OLED is, therefore, of general importance to improving device efficiency.

In this study, we focus on whether the formation of exciplexes in an operating LED may in some way be associated with nitrogen containing moieties. A specific role of the nitrogen nonbonding orbital in the formation process for excimer and exciplexes has previously been reported by De Lucia et al. for molecules such as poly(*p*-pyridine), poly(*p*-pyridyl vinylene), and poly(*N*-vinylcarbazole).[26] Accordingly, we use an alternating copolymer of carbazole and pyridine as workhorse for our investigation [Fig. 1(a)]. Both units are well investigated, simple, and frequently used as building blocks for hole-transport materials. The use of an alternating copolymer ensures that there are a high number of sites with a carbazole unit adjacent to a pyridine unit. Of course, the insights gained from this copolymer model system should apply in an analogous fashion to molecular heterojunctions formed in blends or bilayers of distinct hole-transport and electron-transport molecules. On the basis of luminescence spectroscopy and quantum chemical calculations, we suggest that, in this copolymer, electroplex formation occurs preferentially via a precursor state, that is, a charged complex that only forms under device operation.

EXPERIMENTAL

The polymer Car-Py has been synthesized according to the literature method.[27,28] The Suzuki polycondensation of 2,5-dibromo-4-octylpyridine with 3,6-bis(4,4,5,5-tetramethyl-1,3,2-dioxaboralane)-9-octylcarbazole was carried out by using palladium (II) acetate (2 mol %), tricyclohexylphosphine, and tetraethylammonium hydroxide (20% aqueous solution) in toluene as catalyst system, and end-capped with bromobenzene and phenylboronic acid to afford the desired copolymer Car-Py.

Details and results of the synthetic procedure are as follows. To a flame-dried Schlenk tube, 2,5-dibromo-4-octylpyridine (98.6 mg, 0.28 mmol), 3,6-bis(4,4,5,5-tetramethyl-1,3,2-dioxaboralane)-9-octylcarbazole (150 mg, 0.28 mmol), palladium (II) acetate (1.3 mg, 0.006 mmol), and tricyclohexylphosphine (6.3 mg, 0.022 mmol) were degassed and 1-mL distilled toluene was added. The mixture was heated at 90 °C under nitrogen for half an hour before the degassed tetraethylammonium hydroxide (2.0 mL, 2.8 mmol) was added, and the resulting mixture was stirred at 90 °C under nitrogen overnight. Bromobenzene (0.03 mL, 0.28 mmol) was added and stirred for an hour before phenylboronic acid (34 mg, 0.28 mmol) was added and stirred for another hour to end-cap the polymer. The biphasic mixture was cooled down to room temperature and poured into 100-mL MeOH and stirred for half an hour. The precipitate formed was filtered and redissolved in $CHCl_3$ and passed through a short silica column. Reduction of solvent gave a yellow oil, which was added dropwise to 50-mL methanol with constant stirring. The solid was filtered and redissolved in $CHCl_3$ and precipitated the polymer from 50-mL MeOH. The solid was filtered and dried under vacuum afforded a pale yellow powder (64 mg, 48.9%).

^{1}H NMR (500 MHz, $CDCl_3$): δ 0.75–0.87 (bm, CH_3), 1.14–1.96 (bm, CH_2), 2.65–2.80 (bm, CH_2), 4.00–4.39 (bs, N—CH_2), 7.26–7.52 (bm, ArH), 7.83–7.87 (bm, ArH), 8.11 (bs, ArH), 8.22–8.32 (bm, ArH), 8.67 (bs, ArH). ^{13}C NMR (125 MHz, $CDCl_3$): δ 14.1, 22.6, 27.4, 29.1, 29.2, 29.4, 29.7, 31.8, 109.0, 119.0, 123.6, 125.5, 133.2, 139.9.

Optical measurements were carried out both on solutions and on thin films. Films of about 90 nm thickness were produced by spin-coating the copolymers from toluene solution (10 mg/mL) on a quartz substrate (Spectrosil B). For concentration-dependent solution measurements, toluene was used as solvent with copolymer concentrations from 10^{-6} mol/L to 10^{-3} mol/L, where "mol" refers to one repeat unit of the copolymer. To vary the polarity of the solvent, toluene, methylcyclohexane, and a 1:1 mixture of both were used as solvents with copolymer concentrations of 10^{-3} mol/L. For absorption measurements, a Hewlett-Packard ultraviolet–visible spectrometer was used. For the photoluminescence (PL) measurements, excitation was provided using the tripled output at 355 nm of a Nd:YAG laser operated at 10 Hz (pulse width 6 ns) or using the 355 nm and 365 nm lines of a continuous wave Argon-ion laser. For detection of steady-state spectra, a charge coupled device (CCD) camera (Andor iDus DU420) connected to a spectrograph (Oriel MS125) was used. Time-resolved spectra were obtained with an intensified CCD camera (Andor iDus DU420) adjoint to a (Oriel MS125) spectrograph. All thin film measurements were carried out with the sample in a continuous flow Helium cryostat that was either evacuated or filled with a small amount of exchange gas. The temperature of the sample was controlled using an Oxford Intelligent temperature controller (ITC502).

For the theoretical analysis, we used two types of model systems. We considered (i) the interaction of an isolated carbazole unit with an isolated pyridine unit [Fig. 1(b)] and (ii) the interaction between two dimers [with 2 pyridines and 2 carbazoles on each molecule, as shown in Fig. 1(c)]. All the calculations have been made with density functional theory (DFT) using the ωb97xd functional and a SVP basis set available within the Gaussian 09 package.[29] In parallel, calculations have been made using the constrained DFT (C-DFT) method,[30] implemented within NWChem,[31] which allows to constrain charges on a specific molecule and thereby appears as an appealing tool to model the formation of an electroplex. For these calculations, the B3LYP functional has been used (as the ωb97xd functional has not been implemented yet in NWChem) together with the 6-31G basis set. To shed light into the nature of the relevant electronic states, charge distributions have been computed using the Hirshfeld analysis method.[32]

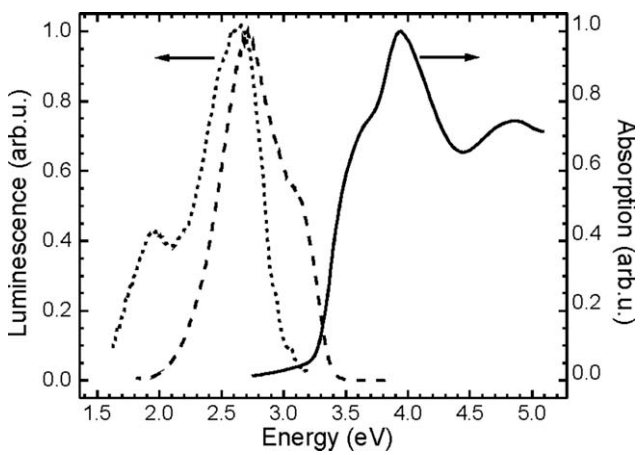

FIGURE 2 Thin film absorption (solid line), photoluminescence (dashed line), and electroluminescence (dotted line) of Car-Py, normalized to unity.

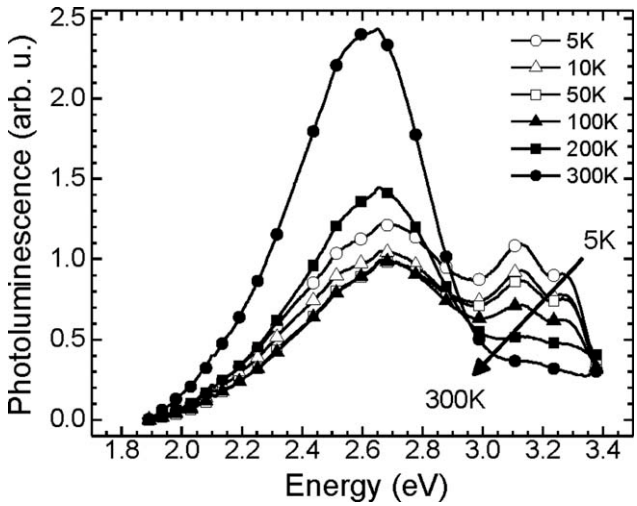

FIGURE 3 Photoluminescence spectra of Car-Py taken on a thin film as a function of temperature.

RESULTS

Optical Measurements

The absorption, PL, and electroluminescence (EL) spectra of the copolymer are shown in Figure 2. The absorption has an onset at 3.25 eV, a shoulder at about 3.60 eV, and a peak at 3.95 eV. The PL spectrum consists of two poorly resolved bands at 3.1 eV and 2.7 eV together with a small unresolved red tail. The EL spectrum shows marked differences to the PL. The high energy feature at 3.1 eV in PL is not present in EL. The intense broad featureless peak is slightly shifted from 2.7 eV in PL to 2.6 eV in EL. Most importantly, there is an additional broad unstructured emission centered at 1.95 eV that only occurs for electrical excitation. To clarify the origin of the three bands centered at 3.1 eV, at about 2.7 eV, and at 1.95 eV, we have investigated the temperature dependence of the PL spectra. This is displayed in Figure 3.

We observe a different temperature dependence for the band at 3.1 eV compared to the peak at 2.7 eV. At 5 K, the 3.1 eV band shows some structure and it is of approximately equal intensity to the band at 2.7 eV. With increasing temperature, the 3.1 eV band disappears, whereas the band at 2.7 eV increases. The different temperature dependence of the bands at 3.1 eV and at 2.7 eV implies that they are caused by different electronic transitions. This is further supported by the different emission lifetimes of both bands. Figure 4 shows the PL as a function of time for different

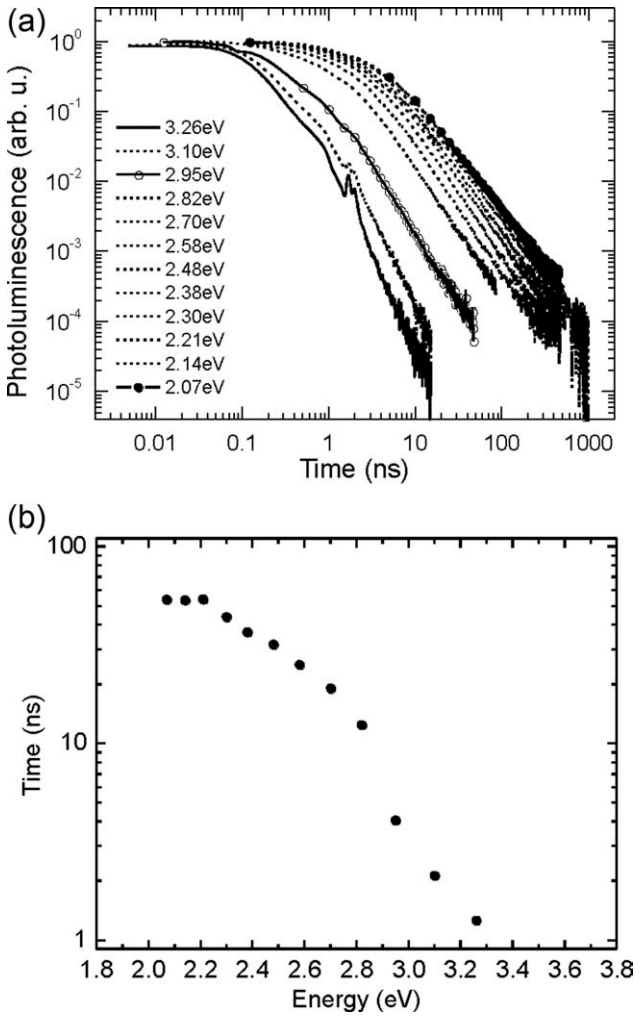

FIGURE 4 (a) Decay of the thin film photoluminescence intensity at 300 K with time for different emission energies. (b) Time until the 300 K photoluminescence intensity of a thin film is reduced to 1% of its initial value as a function of emission energy.

emission energies taken at room temperature. The emission is multiexponential, implying a distribution of lifetimes. Nevertheless, one can observe that the 3.1 eV band decays faster than the energy band at 2.7 eV. In the spectral range of 2.95–3.26 eV, the PL decays to 1% of its initial intensity in about 1–4 ns, whereas about 20–60 ns are required for the same decay in the spectral range from 2.82 eV downward.

To identify the origin of these two states, we measured the PL in different solvents and with different concentrations. The concentration-dependent spectra [Fig. 5(a)] taken in toluene solution show that the peak at 2.7 eV disappears when the concentration is reduced. This implies that the excited state involved in the 2.7 eV transition has an interchain origin, whereas the higher energetic band at 3.1 eV can be assigned to an intrachain excited state. Measurements in solvents with different polarity were carried out to check whether there is some charge transfer character to one of the excited states. As a less polar alternative to toluene, methylcyclohexane was chosen as well as a mixture (1:1) from both solvents with a resulting intermediate polarity. The spectra obtained [Fig. 5(b)] show a small hypsochromic shift with reduced solvent polarity implying a slightly polar character for the 3.1 eV band.

The results presented in Figures 3–5 lead us to conclude that the PL is due to emission from two different excited states. The state at about 3.1 eV is of an intrachain origin and has a slightly polar nature, whereas the state centered at 2.7 eV involves interchain interactions. The emission centered at 2.6 eV in the EL spectrum has an approximately similar width and shape than the 2.7 eV PL band. It is, therefore, likely to be of the same interchain origin. The occurrence of the additional low-energy peak centered at 1.95 eV only for electrical excitation implies that the presence of an unpaired charge carrier is a necessary condition for either the observation or the formation of this state.

We now focus on identifying the formation pathway for the low-energy emission band centered at 1.95 eV. Even though there are frequent reports on the observation of electromers or electroplexes,[14–22] it is not well understood why these states are only observed for electrical, yet not for optical excitation.

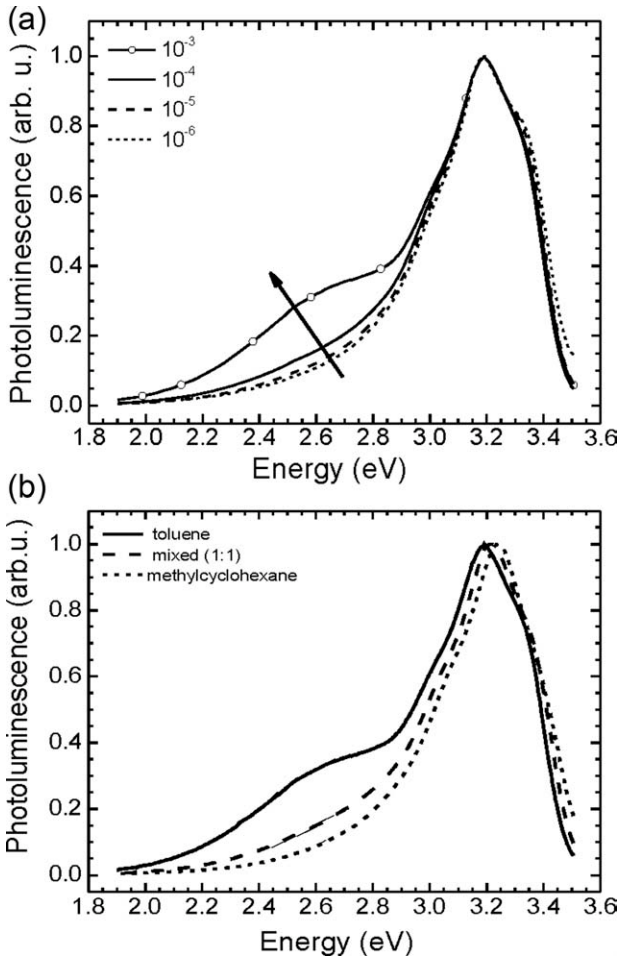

FIGURE 5 (a) Photoluminescence (300 K) in solution as a function of concentration in toluene. Concentrations are in units of mol/L, where mol refers to one repeat unit. The arrow indicates increasing concentration. (b) Photoluminescence (300 K) in solution for different solvents, at 10^{-3} mol/L.

One possible explanation consists in considering electroplexes as the tail states of an exciplex distribution that is populated more efficiently for electrical excitation. It is certainly true that a small fraction of low-energy sites will always feature more prominently in EL than in PL.[33] Electrically injected charge carriers probe a large area of the film before they recombine. This implies that they also probe a large part of the available density of states. As a consequence, they relax very efficiently to any low-energy sites that are present in the film. In contrast, optical excitation creates excitons at any site in the film, and only relatively nearby low-energy sites are reached by energy transfer during the lifetime of the state. Consequently, low energy trap-like states appear in general more prominently for EL.[33]

However, the material we consider here is a copolymer that, by its nature, forms many internal interfaces where a carbazole moiety is adjacent to a neighboring pyridine unit. At least some of these sites with a suitable geometry should be within the diffusion range of an exciton. The complete absence of any, even weak, emission feature in PL at 1.95 eV is suspicious, even more so because the peak at 2.6/2.7 eV is present for both, optical and electrical excitation. It raises the question whether a suitable geometry for the 1.95 eV exciplex formation may not be obtained by optical excitation. Because the 1.95 eV emission is seen for electrical excitation, we conjecture that unpaired charge carriers may play a role in bringing about a suitable precursor geometry, from which the 1.95 eV exciplex formation can take place.

For many nitrogen-containing moieties such as carbazoles or triphenylamines,[34,35] a positive charge tends to localize around the lone pair of a nitrogen. This suggests that the nitrogen lone pair should have a key role in the exciplex formation process. If we consider existing literature, a specific role of nitrogen has been suggested by a number of authors. On the basis of luminescence measurements on polyvinylcarbazole and a pyridine-containing polymer, De Lucia et al. suggest an exciplex formation scheme that involves an interaction between a nonbonding molecular orbital of the pyridine-containing polymer and the delocalized π-orbital of the polyvinylcarbazole.[26] It should be noted that they neglect any contribution from the nonbonding orbitals in the carbazole-moiety.

Lewis et al. invoke a nitrogen–nitrogen lone pair interaction to explain exciplex formation in combination of 9-aminophenanthrene or 3-aminostilbene as first component and small amines as second component. Specifically, they consider a Lewis-acid-base interaction between the lone-pair donor (the ground-state amine) and the lone-pair acceptor (the excited aminophenanthrene).[36] In their picture, the excited aminophenanthrene has a positive charge initially localized on the nitrogen lone orbital, whereas the negative charge is delocalized on the phenyl rings. This excited aminophenanthrene then interacts with a ground state amine that serves as a lone-pair donor. As a result, the positive charge is delocalized over both amines, with the negative charge remaining on the phenyl rings. Similar observations have been made by Chandros and Thomas[37] for intramolecular exciplexes of naphthylalkylamines.

The stabilization of positive charges localized on a nitrogen lone pair by interacting with a further lone pair from a ground state amine has been described in the literature: Theoretical studies have shown that the ammonia radical cation (where the positive charge is localized on the nitrogen lone pair) can be stabilized through the formation of a specific two-centre three-electron bond with a lone pair from, for example, an imine nitrogen atom.[38] Experimentally, the formation of a two-centre-three-electron bond between the nitrogen atoms of the two methyl groups in the excited state of 1,8-bis(dimethylamino)naphthalene has been found responsible for the drastic geometry change upon excitation.[39]

We have performed quantum chemical calculations to address two issues. First, we want to see whether the presence of a charge in the polymer brings about an attractive interaction between two adjacent chains, such that a precursor complex develops with a geometry that favors subsequent exciplex formation. Second, considering the just mentioned body of work, we want to find out whether a specific nitrogen–nitrogen interaction between a charged and a neutral molecule may also exist for the Car-Py polymer.

Quantum-Chemical Modeling

Singly Charged Precursor State

To assess the effect of a charge on the interactions between two neighboring polymer chains, we consider a model system comprising two adjacent dimers as shown in Figure 1(c). Each dimer consists of two carbazole and two pyridine units, so that in the middle of the dimer both the carbazole and the pyridine unit are connected from both sides to the respective other unit. Because donor–acceptor copolymers show limited conjugation, the dimer should closely resemble the Car-Py polymer as far as the excited-state electronic structure is concerned.

Before studying the interaction between two dimers, it is instructive to consider the charge distribution and the geometry of an individual dimer in its neutral ground state as well as in the presence of an excess positive or negative charge. We optimized the geometry for the neutral, positively, and negatively charged dimer and performed a Hirshfeld charge distribution analysis in each case. Figure 6(a) shows the partial charges per repeating units, whereas Figure 6(b) lists the corresponding dihedral angles between adjacent units. All data shown in Figure 6 is also available as tables in the supporting information. In the neutral molecule, a small amount of negative charge density is found on the central pyridine unit Py2 and a similar small amount of positive charge density on the central carbazole Car1, see Figure 1(c) for labeling. There is significant torsion between the central pyridine and carbazole, Py2 and Car1, with a dihedral angle of 57°. The dihedral angles to the outer units, that is, from Car2 to Py2 and from Car1 to Py1, are smaller. When an electron is removed from the dimer, that is, in the presence of a positive charge, the molecule planarizes significantly, with a dihedral angle of only 36° between Py2 and Car1. The positive charge density spreads over the entire dimer, yet with larger contributions on the carbazole moieties. In contrast, a negative charge localizes on the Car1 and Py1 sites, with the angle between the

two units being 0°, whereas all other angles are as for the neutral molecule.

We next consider how this charge distribution is affected by the presence of a second polymer chain here modeled as another dimer. The arrangement and labeling of the two dimers is indicated in Figure 1(c), whereas Figure 6(c) illustrates the distribution of charges on the different units of the dimer pair. As for the single dimer, the geometric structure of the dimer pair in the neutral and charged states has been optimized and the associated charge distribution analyzed. For the neutral pair of dimers, the charge distribution is the same as for the isolated dimer, with some positive charge density on the carbazole site and some negative charge density on the pyridine site.

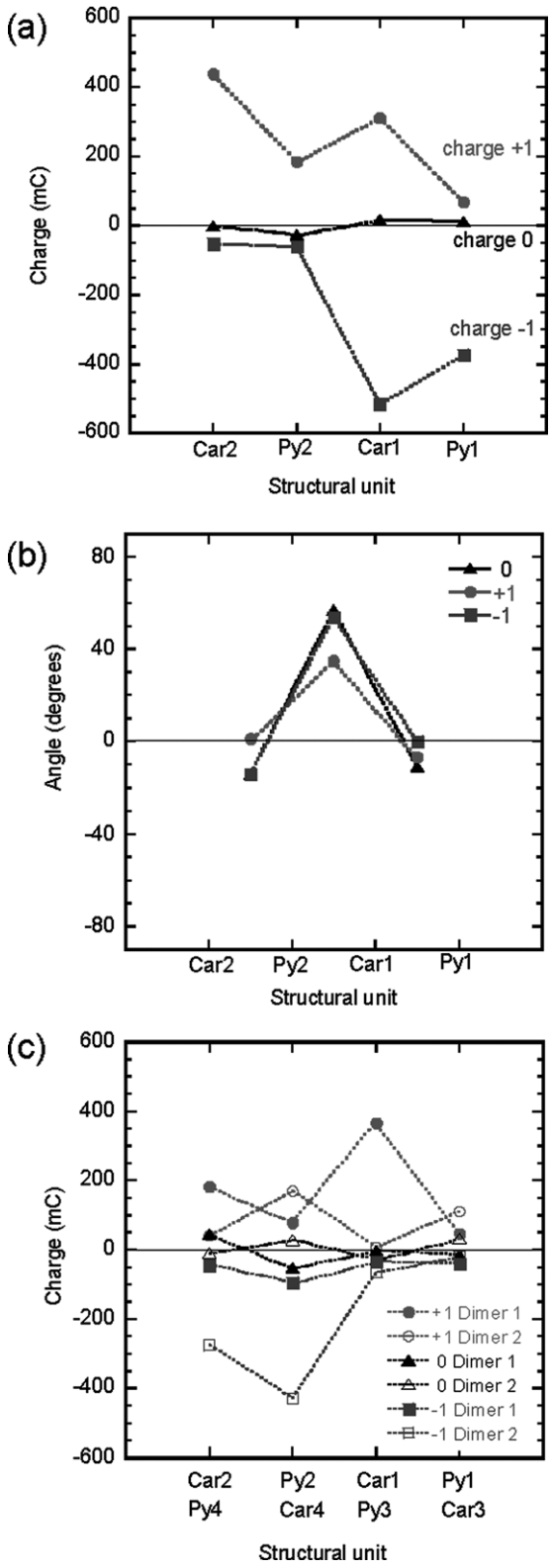

When a single positive charge is distributed over the two-chain system, we find that it localizes mostly on the Car1 unit, although there is also a non-negligible part of positive charge on the other carbazole units. Furthermore, there is a lower fraction of positive charge on the pyridine units in the pair arrangement than in the isolated molecule. In the isolated positively charged dimer, the amount of charge on the pyridine units adds up to 25% of the total charge, whereas it sums up to only 17% in the dimer pair. This implies that the presence of a second dimer affects the charge distribution such that the carbazole moieties become more positively charged. This suggests significant quantum-mechanical coupling between the two chains. We also note that, in the low-symmetry geometric configurations considered here, the charge density is neither located entirely on only one of the dimers nor is it distributed equally within the pair. It turns out that 67% of the positive charge is located on one dimer and 33% on the other. Similarly, in the negatively charged dimer pair, 79% of the charge is born by one of the dimers. Yet, in contrast to the positively charged case, the charge distribution in the pair closely resembles that of the isolated molecule, that is, with the excess electron density essentially localized on one carbazole–pyridine unit, thus possibly pointing to a weaker intermolecular interaction.

It is instructive to consider the equilibrium distance between the nitrogen atoms on adjacent dimers, listed in Table 1. NN1 refers to the distance between the nitrogen of Py2 and the nitrogen of Car4, and NN2 is the distance from the carbazole nitrogen in Car1 to the pyridine nitrogen in Py3 (see Fig. 1). When the pair is neutral, the nitrogen–nitrogen distances between the center moieties, NN1 and NN2, are similar and around 3.5 Å. For the negatively charged pair, the nitrogen atoms seem to slightly repel each other, with namely a larger equilibrium distance of 3.6 Å for NN1 where most of the negative charge is located. Quite in contrast to this, the distance between nitrogens reduces for the positively charged dimer,

FIGURE 6 (a) Distribution of a positive or negative charge of 1 C over the units of one dimer as labeled in Figure 1. (b) Torsion angle between adjacent units of one dimer. (c) Distribution of a positive or negative charge of 1 C for the units on the dimer pair as labeled in Figure 1. Black triangles refer to the neutral dimer, red circles to the positively charged dimer, and blue squares to the negatively charged dimer, respectively. In (c), full (open) symbols refer to the units of dimer 1 (2) in the dimer pair, as denoted by the top (bottom) row of the label. Dotted lines are guides to the eye.

TABLE 1 Intermolecular Distances and Interaction Energies for Two Adjacent Dimers [cf. Fig. 1(c)]

Total Charge (C)	NN1 (Py2-Car4)	NN2 (Car1-Py3)	ΔE (eV)
+1	3.307 Å	3.248 Å	−2.35
0	3.544 Å	3.552 Å	−2.00
−1	3.587 Å	3.554 Å	−1.99

The columns NN1 and NN2 list the distance between nitrogen atoms on neighboring dimers as a function of the total charge of the system. These distances are calculated using the DFT method with the ωb97xd functional and SVP basis set. ΔE gives the interaction energy as a function of the total charge of the system. This is calculated as the difference between the total energy of the pair minus the total energy of each single dimer. The total charge 0 refers to two neutral adjacent dimers.

with NN1 being 3.3 Å and NN2 (where a larger amount of positive charge is located) taking a value of 3.2 Å. Thus, this comparison of equilibrium geometries indicates that a positive charge on a pair results in a closer nitrogen–nitrogen distance compared with a neutral or negatively charged pair. This trend is confirmed by the pair binding energies, computed as the difference between the total energy of the neutral (charged) pair minus the total energy of each single neutral (charged) dimer molecule. As observed in Table 1, this interaction energy is significantly larger for the positively charged system. Adding a positive charge to one polymer chain (here a dimer) thus results in a significant rearrangement of the supramolecular geometric structure (namely a shorter interchain distance) as well as electronic structure (redistribution of the electronic density, *vide supra*). This is accompanied by a larger interaction energy. Such effects highlight resonance interactions between adjacent chains. Thus, the DFT calculations strongly support the formation of a positively charged complex that may act as a precursor state to an exciplex.

Electroplex State

As a next step in our modeling study, we focus on the modeling of the formation of the electroplex through the precursor charged state. This requires assigning excess positive and negative charges to molecular fragments, which can be handled using constrained DFT. Because of size limitations, we restrict our investigations here to single carbazole and pyridine units initially interacting in a cofacial arrangement. These structures are then subjected to geometry optimization with specific constraints on the charge distribution. In practice, as inspired by the DFT calculation in the previous section, we assign (i) a positive charge to carbazole and a negative charge to pyridine to model the electroplex; (ii) a positive charge on the carbazole and a neutral pyridine to model the charged precursor state; and (iii) both molecules in their uncharged state for the neutral pair ground state. The final structures obtained after geometry optimization, as well as the potential energy curves as a function of NN distance, are displayed in Figure 7.

It is evident that the presence of the positive charge decreases the NN distance, and, moreover, the charge also affects the molecular orientation. Like for the dimers, the potential energy curve has a minimum at shorter NN distance for the positively charged system (3.06 Å) than for the neutral system (3.38 Å). The interaction energy, derived in the same way as for the dimers, is presented in Table 2. As for the dimer pair, it shows that the presence of the positive charge favors the interaction. The higher interaction energy, shorter NN distance, and in particular the change in orientation strongly suggest that the attractive interaction between the carbazole and the (neutral) pyridine is associated with interactions between the nitrogen atoms. Note that for the pyridine, the lone pair is in the plane of the molecule, like a σ-orbital, whereas for the (neutral) carbazole, the nitrogen lone pair is orthogonal to the molecular plane like a π-orbital. The molecular reorientation may thus assist in increasing orbital overlap. When a negative charge is added, the NN distance decreases significantly to

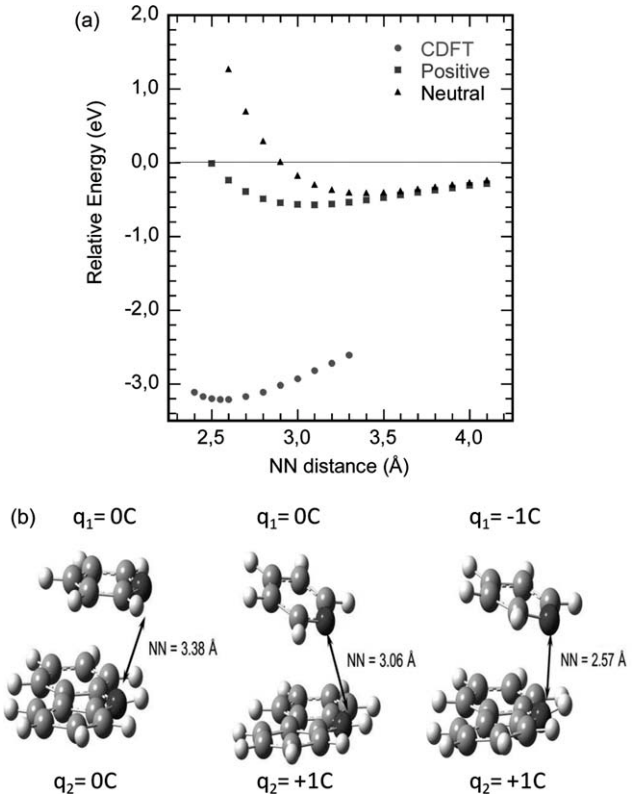

FIGURE 7 (a) Potential energy curve for a pyridine and a carbazole unit as a function of the distance between the nitrogen atoms for the neutral system (in the ground state), the positively charged system and the system with a positive charge on the carbazole and a negative charge on the pyridine (C-DFT). The potential energy curve has been obtained by first optimizing the geometry and then moving the molecules along their connecting N-N vector with an otherwise unchanged geometry. The potential energy curves are placed vertically so that their minima indicate interaction energy (cf. Table 2). (b) Structures after geometry optimization. The neutral and positively charged systems have been optimized using the ωb97xd functional within Gaussian 09. The system with a positive charge on the carbazole and a negative on the pyridine has been optimized using the C-DFT method with B3LYP functional as implemented in NWCHEM.

TABLE 2 Intermolecular Distances and Interaction Energies for a Pyridine Adjacent to a Carbazole [cf. Fig. 1(b)]

Total Charge (C)	NN (Å)	ΔE (eV)
+1 (DFT)	3.064	−0.57
0 (DFT)	3.381	−0.41
0 (C-DFT)	2.572	−3.21

ΔE gives the interaction energy as a function of the total charge of the system, calculated as described for Table 1. The DFT method with the ωb97xd functional and SVP basis set has been used to for the positively charged system and for the combination of a neutral pyridine next to a neutral carbazole. C-DFT calculations with the B3LYP functional and the 6–31G basis set have been used for the neutral system consisting of a negatively charged pyridine and a positively charged carbazole, listed in the last row of the table. The column NN lists the associated distance between the two nitrogen atoms.

2.572 Å. The structures obtained after geometry optimization is shown in Figure 7(b), where the attraction between the two nitrogen sites is clearly visible.

DISCUSSION AND CONCLUSIONS

On the basis of the luminescence measurements, we have identified a high energy intramolecular state at 3.1 eV with only slightly polar character, an intermolecular state—possibly associated with the ubiquitous π-π interactions—at intermediate energies (2.6/2.7 eV) and a low energy state at 1.95 eV that is only observable for electrical excitation and that we attribute to an electroplex. We propose the following model for the emissive state at 1.95 eV and for its formation pathway in EL: This emissive state is an exciplex that is stabilized by both partial charge transfer and wavefunction overlap. Although this state is energetically more stable than an intrachain exciton (and even more stable than the interchain excited state at 2.6/2.7 eV), it is not formed under optical excitation. In other words, there is insufficient exciton migration to sites with suitable geometry. For electrical excitation, we suggest that a two step process takes place. First, an interchain complex between a positively charged and a neutral segment on neighboring chains is formed. The charged intermolecular complex is of a geometry that is very similar to the exciplex geometry. In a second step, an electron gets trapped on the positively charged complex and an excited state complex, that is, an exciplex, is formed. EL occurring from this state is responsible for the additional red-shifted emission detected in EL.

Evidence in support for this model comes from the quantum chemical calculations.

i. We have shown that a positive charge causes an attractive interaction between two neighboring dimers that is associated with a shorter intermolecular distance than for the neutral or negatively charged dimer pair. This positive charge is mainly localized on the carbazole units. In other words, a positive charge causes the formation of a positively charged complex.

ii. We have shown that the equilibrium intermolecular distance reduces further when a negatively charged pyridine is opposite to a positively charged carbazole. This system represents an exciplex. Thus, the complex formed in the presence of a positive charge can be considered as a precursor to an exciplex.

iii. For the positively charged dimer pair, the charge is not localized on only one dimer, but rather, on average, the charge is distributed over both dimers. Clearly, the hole is not "split" but it oscillates back and forth between both dimers, thus implying some resonance character. Furthermore, the equilibrium structures of the positively charged pyridine–carbazole complex and of the exciplex show a strong tilt of the nitrogen atoms toward each other, suggesting a specific interaction of the nitrogen atoms with each other, possibly through the nonbonding orbitals.

The model we have suggested here extends commonly held views on electroplexes in two ways. First, by proposing the involvement of a charged precursor state, we go beyond the perception that electroplexes are formed in EL merely because the relevant sites become populated more efficiently. The formation of such a charged precursor—essentially a trapped hole—is consistent with observations made by other groups. For example, the Cambridge group has recently shown that the presence of ions can also serve to stabilize charge-transfer excitations in a F8BT, a copolymer consisting of fluorene and benzothiadiazole units.[40] Similarly, for a carbazole-modified polyfluorene, it was noted that a dimer formed by two carbazoles can act as a hole trap so that it becomes a stable radical cation after catching a hole. Electroplex formation in the carbazole-modified polyfluorene is then attributed to a recombination of this radical cation with a nearby radical anion main chain fluorene segment with a proper orientation.[19] Second, by proposing the involvement of the nitrogen nonbonding orbital, we go beyond the usual concept of a charge-transfer state. In this way, our model adds to the earlier works of De Lucia et al.,[26] Lewis et al.,[36] Humbel et al.,[38] and Balkowski et al.[39]

Given the frequent use of nitrogen-containing chromophores such as carbazole-moieties, amine-moieties, or oxadiazole-moieties as charge transport materials and the similarly frequent occurrence of electroplex formation in these compounds, it would be desirable to explore whether the model suggested here is specific to only a few carbazole and pyridine containing compounds, or whether it is applicable more widely to materials with nitrogen containing moieties. In general, exciplexes are detrimental for OLEDs due to their low luminescence quantum yields and knowing what causes them is the first step to prevent their formation. For some compounds, however, such as F8BT/TFB (both compounds with nitrogen containing moieties), the energy gap between exciplex and exciton is very small. In that case, thermal excitation leads to exciton formation from the exciplex state. Gaining insight into the mechanism of exciplex formation for electrical excitation then becomes central to understanding OLED operation.

Our model contains two elements, the formation of a precursor state, and a specific N-N interaction. Clearly, the possible need for a precursor state formed by electrical excitation will depend on factors such as the particular molecular geometries, reorganization energies for exciplex formation and the polarity of the S_1

excited state. These parameters will be material dependent. In the light of our results and the works by De Lucia et al., Lewis et al., Humbel et al., and Balkowski et al., it would furthermore be interesting to consider whether specific nitrogen–nitrogen interactions contribute to some of the exciplexes that are frequently observed for optical excitation in other nitrogen-containing chromophores. When the partial localization of the positive charge in S_1 is strong enough, an interaction between the neighboring nitrogen containing sites, involving the nitrogen lone pair, may also take place for optical excitation.

ACKNOWLEDGMENTS

The authors thank A. Holmes (University of Cambridge, UK and University of Melbourne, Australia) for his support, advice, and interest. C. S. K. Mak acknowledges support by the Croucher Foundation and the EU (STEPLED). A. Köhler thanks the DFG for support through the GRK 1640. The work in Mons was supported by the Interuniversity Attraction Pole Program of the Belgian Federal Science Policy Office (PAI 6/27), FNRS-FRFC, the EC 7th Framework Program under Grant Agreement No. 212311 of the ONE-P Project, and the Graduiertenkolleg 1640 of the DFG. D. Beljonne is a FNRS Research Director.

REFERENCES AND NOTES

1 Peet, J.; Kim, J. Y.; Coates, N. E.; Ma, W. L.; Moses, D.; Heeger, A. J.; Bazan, G. C. *Nat. Mater.* **2007,** *6*, 497–500.

2 Ballantyne, A. M.; Chen, L.; Dane, J.; Hammant, T.; Braun, F. M.; Heeney, M.; Duffy, W.; McCulloch, I.; Bradley, D. D. C.; Nelson, J. *Adv. Funct. Mater.* **2008,** *18*, 2373–2380.

3 Solomeshch, O.; Yu, Y. J.; Goryunkov, A. A.; Sidorov, L. N.; Tuktarov, R. F.; Choi, D. H.; Jin, J. I.; Tessler, N. *Adv. Mater.* **2009,** *21*, 4456–4460.

4 Li, Y. Q.; Mastria, R.; Fiore, A.; Nobile, C.; Yin, L. X.; Biasiucci, M.; Cheng, G.; Cucolo, A. M.; Cingolani, R.; Manna, L.; Gigli, G. *Adv. Mater.* **2009,** *21*, 4461–4466.

5 Yin, C.; Kietzke, T.; Neher, D.; Hörhold, H. H. *Appl. Phys. Lett.* **2007,** *90*, 092117.

6 Yin, C. H.; Kietzke, T.; Kumke, M.; Neher, D.; Hörhold, H. H. *Sol. Energy Mater. Sol. Cells* **2007,** *91*, 411–415.

7 Kietzke, T.; Hörhold, H. H.; Neher, D. *Chem. Mater.* **2005,** *17*, 6532–6537.

8 Veldman, D.; Meskers, S. C. J.; Janssen, R. A. J. *Adv. Funct. Mater.* **2009,** *19*, 1939–1948.

9 Reineke, S.; Lindner, F.; Schwartz, G.; Seidler, N.; Walzer, K.; Lussem, B.; Leo, K. *Nature* **2009,** *459*, 234–238.

10 Sun, Y. R.; Giebink, N. C.; Kanno, H.; Ma, B. W.; Thompson, M. E.; Forrest, S. R. *Nature* **2006,** *440*, 908–912.

11 Morteani, A. C.; Dhoot, A. S.; Kim, J. S.; Silva, C.; Greenham, N. C.; Murphy, C.; Moons, E.; Cina, S.; Burroughes, J. H.; Friend, R. H. *Adv. Mater.* **2003,** *15*, 1708–1712.

12 Jenekhe, S. A.; Osaheni, J. A. *Science* **1994,** *265*, 765–768.

13 Morteani, A. C.; Sreearunothai, P.; Herz, L. M.; Friend, R. H.; Silva, C. *Phys. Rev. Lett.* **2004,** *92*, 247402.

14 Giro, G.; Cocchi, M.; Kalinowski, J.; Di Marco, P.; Fattori, V. *Chem. Phys. Lett.* **2000,** *318*, 137–141.

15 Granlund, T.; Pettersson, L. A. A.; Anderson, M. R.; Inganas, O. *J. Appl. Phys.* **1997,** *81*, 8097–8104.

16 Wang, Y. M.; Teng, F.; Xu, Z.; Hou, Y. B.; Wang, Y. S.; Xu, X. R. *Eur. Polym. J.* **2005,** *41*, 1020–1023.

17 Zhao, D. W.; Xu, Z.; Zhang, F. J.; Song, S. F.; Zhao, S. L.; Wang, Y.; Yuan, G. C.; Zhang, Y. F.; Xu, H. H. *Appl. Surf. Sci.* **2007,** *253*, 4025–4028.

18 Zhao, D. W.; Zhang, F. J.; Xu, C.; Sun, J. Y.; Song, S. F.; Xu, Z.; Sun, X. W. *Appl. Surf. Sci.* **2008,** *254*, 3548–3552.

19 Liao, J. L.; Chen, X. W.; Liu, C. Y.; Chen, S. A.; Su, C. H.; Sut, A. C. *J. Phys. Chem. B* **2007,** *111*, 10379–10365.

20 Zhang, F. J.; Zhao, S. L.; Zhao, D. W.; Jiang, W. W.; Li, Y.; Yuan, G. C.; Zhu, H. N.; Xu, Z. *Phys. Scr.* **2007,** *75*, 407–410.

21 Yang, S. Y.; Zhang, X. L.; Hou, Y. B.; Deng, Z. B.; Xu, X. R. *J. Appl. Phys.* **2007,** *101*, 096101.

22 Yang, C. C.; Hsu, C. J.; Chou, P. T.; Cheng, H. C.; Su, Y. O.; Leung, M. K. *J. Phys. Chem. B* **2010,** *114*, 756–768.

23 Finlayson, C. E.; Kim, J. S.; Liddell, M. J.; Friend, R. H.; Jung, S. H.; Grimsdale, A. C.; Müllen, K. *J. Chem. Phys.* **2008,** *128*, 044703.

24 Jenekhe, S. A. *Adv. Mater.* **1995,** *7*, 309–311.

25 Benson-Smith, J. J.; Wilson, J.; Dyer-Smith, C.; Mouri, K.; Yamaguchi, S.; Murata, H.; Nelson, J. *J. Phys. Chem. B* **2009,** *113*, 7794–7799.

26 De Lucia, F. C.; Gustafson, T. L.; Wang, D.; Epstein, A. J. *Phys. Rev. B* **2002,** *65*, 235204.

27 Towns, C. R.; O'Dell, T. PCT Int Appl WO 053,656 A1, **2000.**

28 Rees, I. D.; Robinson, K. L.; Holmes, A. B.; Towns, C. R.; O'Dell, R. *MRS Bulletin* **2002,** *27*, 451–460.

29 Frisch, M. J.; Trucks, G. W.; Schlegel, H. B.; Scuseria, G. E.; Robb, M. A.; Cheeseman, J. R.; Scalmani, G.; Barone, V.; Ismaylov, B. A. F.; Bloino, J.; Zheng, G.; Sonnenberg, J. L.; Hada, M.; Ehara, M.; Toyota, K.; Fukuda, R.; Hasegawa, J.; Ishida, M.; Nakajima, T.; Honda, Y.; Kitao, O.; Nakai, H.; Vreven, T.; Montgomery, J. A., Jr.; Peralta, J. E.; Ogaliaro, F.; Bearpark, M.; Heyd, J. J.; Brothers, E.; Kudin, K. N.; Staroverov, N. N.; Kobayashi, R.; Normand, J.; Raghavachari, K.; Rendell, A.; Burant, J. C.; Iyengar, S. S.; Tomasi, J.; Cossi, M.; Rega, N.; Millam, J. M.; Klene, M.; Knox, J. E.; Cross, J. B.; Bakken, V.; Adamo, C.; Jaramillo, J.; Gomperts, R.; Stratmann, R. E.; Yazyev, O.; Austin, A. J.; Cammi, R.; Pomelli, C.; Ochterski, J. W.; Martin, R. L.; Morokuma, K.; Zakrzewski, V. G.; Voth, G. A.; Salvador, P.; Dannenberg, J. J.; Dapprich, S.; Daniels, A. D.; Farkas, Ö.; Foresman, J. B.; Ortiz, J. V.; Cioslowski, J.; Fox, D. J. Gaussian 09, Revision A1; Gaussian, Inc.: Wallington CT, **2009.**

30 Wu, Q.; Van Voorhis, T. *Phys. Rev. A* **2005,** *72*, 024502.

31 Valiev, M.; Bylaska, E. J.; Govind, N.; Kowalski, K.; Straatsma, T. P.; van Dam, H. J. J.; Wang, D.; Nieploch, J.; Apra, E.; Windus, T. L.; de Jong, W. A. *Comput. Phys. Commun.* **2010,** *181*, 1477–1489.

32 Hirshfeld, F. L. *Theor. Chim. Acta* **1977,** *44*, 129–138.

33 Uckert, F.; Tak, Y. H.; Müllen, K.; Bässler, H. *Adv. Mater.* **2000,** *12*, 905–908.

34 Avilov, I.; Marsal, P.; Bredas, J. L.; Beljonne, D. *Adv. Mater.* **2004,** *16*, 1624–1629.

35 Huang, Y. S.; Westenhoff, S.; Avilov, I.; Sreearunothai, P.; Hodgkiss, J. M.; Deleener, C.; Friend, R. H.; Beljonne, D. *Nat. Mater.* **2008,** *7*, 483–489.

36 Lewis, F. D.; Ahrens, A.; Kurth, T. L. *Photochem. Photobiol. Sci.* **2004,** *3*, 341–347.

37 Chandros, E. A.; Thomas, H. T. *Chem. Phys. Lett.* **1971,** *9*, 393–396.

38 Humbel, S.; Hoffmann, N.; Cote, I.; Bouquant, J. *Chem.—-Eur. J.* **2000,** *6*, 1592–1600.

39 Balkowski, G.; Szemik-Hojniak, A.; van Stokkum, I. H. M.; Zhang, H.; Buma, W. J. *J. Phys. Chem. A* **2005,** *109*, 3535–3541.

40 Hodgkiss, J. M.; Tu, G. L.; Albert-Seifried, S.; Huck, W. T. S.; Friend, R. H. *J. Am. Chem. Soc.* **2009,** *131*, 8913–8921.